Proceedings of the XVII ECSMGE-2019
Geotechnical Engineering foundation of the future
ISBN 978-0-7277-6067-8

doi: 17ecsmge-2019-Y-XXXX

XVII European Conference
ECSMGE 2019
Reykjavík
on Soil Mechanics
and Geotechnical Engineering

Comparison of new memory surface hardening models for prediction of high cyclic loading

Comparaison de nouveaux modèles de surface de mémoire à durcissement pour la prévision de fortes charges cycliques

A. Diambra, R. Corti
University of Bristol, Bristol, United Kingdom

H. Y. Liu, F. Pisanò
Delft University of Technology, Delft, Netherlands

J. A. Abell
Universidad de los Andes, Santiago, Chile

ABSTRACT: This paper presents an objective comparison between two recent constitutive models employing the concept of the hardening memory surface to predict the high cyclic loading behaviour of granular soils. The hardening memory surface is applied to the well-known Severn-Trent sand and the SANINSAND04 constitutive models. While the addition of the new model surface (the memory surface) leads to enhanced model capabilities, slight differences in the implementation can lead to different model performances and simulations. This paper describes the differences between the two implementations and highlights the most relevant modelling ingredients to predict particular features of the cyclic soil behaviour. This paper will help the reader in selecting the most suitable model and related ingredients for a particular geotechnical application.

RÉSUMÉ: Cet article présente une comparaison objective entre deux modèles constitutifs récents utilisant le nouveau concept de surface de mémoire à durcissement pour prédire le comportement à forte charge cyclique des sols granulaires. La surface de mémoire durcissante est appliquée au bien connu modèles constitutifs Severn-Trent sand et SANISAND 04. Bien que l'ajout de la nouvelle surface modèle améliore les capacités du modèle, de légères différences dans la mise en œuvre peuvent entraîner des performances et des simulations différentes du modèle. Cet article décrit les différences entre les deux implémentations et met en évidence l'ingrédient de modélisation le plus pertinent pour prédire les caractéristiques particulières du comportement cyclique du sol. Ce document aidera le lecteur à sélectionner le modèle le mieux adapté et les ingrédients associés pour une application particulière.

Keywords: constitutive modelling, cyclic loading, sand, ratcheting, strain accumulation.

1 INTRODUCTION

The accurate prediction of the mechanical response and plastic strain accumulation of granular soils, when subjected to a high number of non-monotonic repeated loads, is a crucial issue for many geotechnical systems. These include offshore systems, railways and earthquake-prone structures among others. Accumulation of permanent cyclic strain may lead to the violation of serviceability limits of the structure. Conversely, excessive generation of pore water pressure during

undrained cycling may lead to reduction of the overall soil capacity/stiffness.

The progressive accumulation of plastic strain during repeated loading is generally denoted by the term 'ratcheting'. Prediction of ratcheting generally relies on empirical relationships calibrated from experimental measurements (e.g. Pasten et al. 2013; Wichtmann 2005). The use of techniques based on full constitutive modelling is unquestionably more time-consuming and demands much higher computing resources. However, such approach would allow a more generalised consideration of all the problem variables including loading amplitude, loading direction, average stress level, soil density and drainage conditions among others.

In this context, the recent memory surface hardening concept in the form proposed by Corti et al. (2016) has shown very successful capabilities for simulating the high-cyclic loading behaviour of granular soils, at the expense of only two additional constitutive parameters. The modelling improvements proposed by Corti et al. (2016) consisted in the introduction of a new model surface – the memory surface – which has the role of retaining information about past stress history and records the effect of continuous cyclic loading. Corti et al. (2016) implemented such feature in the bounding surface, kinematic hardening Severn-Trent sand model (Gajo and Muir Wood, 1999) demonstrating that such addition can allow the simulation of:

- the magnitude and rate of plastic strain accumulation during drained cyclic loading;
- the progressive stiffening of the soil during drained cyclic loading;
- the rate of progressive pore pressure build-up to liquefaction for undrained cyclic loading.

This model was also successfully employed for explaining the cyclic behaviour of sliding foundations and plate anchors (Corti et al. 2017; Chow et al. 2015). The proposal by Corti et al. (2016) has been revisited by Liu et al. (2018a) and the hardening memory surface concept has been implemented in SANISAND04 (Dafalias and Manzari, 2004). Similar performances of those described in Corti et al. (2016) have been obtained, although further improvements were proposed by Liu et al (2018a). Providing an overview of both hardening memory surface models (Corti et al. 2016 and Liu et al. 2018a), this paper presents an objective comparison between them. The aim is to point out the relevant and distinguishable features of each soil model and to describe the respective advantageous traits. It is hoped that such comparison will help the reader in the selection of (i) the most suitable constitutive model and (ii) the most relevant modelling ingredients for their particular geotechnical application.

2 GENERAL CONCEPTS ABOUT MEMORY SURFACE MODELLING

The memory surface is a new model surface which tracks already experienced stress states. As such, when the stress state lies within the memory surface, the soil exhibits a stiffer behaviour. The memory surface acts as an additional bounding surface so that the plastic soil modulus is governed by an additional hardening term depending on the distance between the current stress state and its projection on the memory surface. This enables to reproduce the experimentally observed stiffer soil behaviour during repeated loading if compared to virgin loading. Three rules describe the evolution of the memory surface: (i) the memory surface changes in size because of the experienced plastic strains; (ii) the memory surface always encloses the current stress state; (iii) the memory surface always encloses the current yield surface.

Qualitative examples of the evolution of the memory surface (f^M) are provided in Figure 1 in the π-plane. Circular model surfaces have been adopted for the sake of simplicity, although other surface types will be implemented in the following of this paper. During monotonic

loading the memory surface expands to enclose newly experienced stress states (Fig1a). However, at high stress ratios the memory surface can shrink to simulate a loss of memory (damage of fabric) due to the approaching of critical state conditions (Fig.1b). During non-virgin loading inside the memory surface (i.e. cyclic or repeated loading), the development of plastic strains still leads to an increase of the memory surface (Fig. 1c) which in turn leads to a progressive soil stiffening (i.e. soil stiffening with number of cycles).

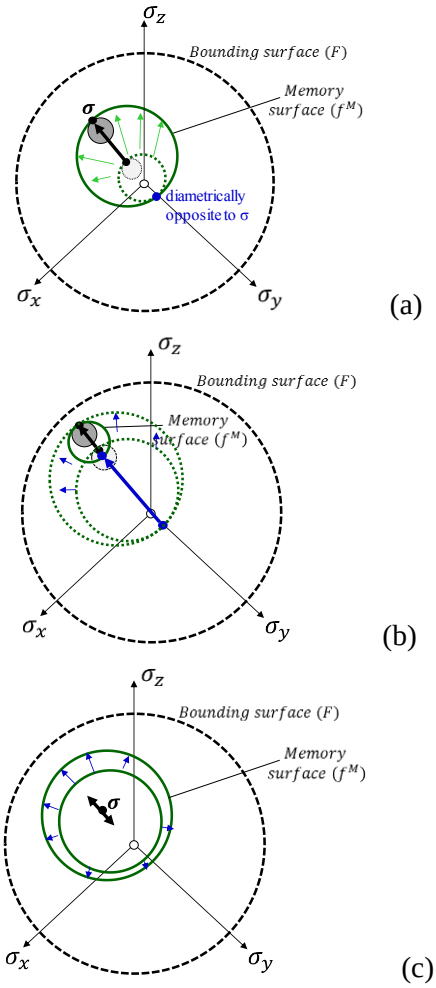

Figure 1 Evolution of the memory surface (f^M): (a) expansion during virgin loading; (b) shrinkage at high stress ratios and (c) expansion during non virgin/cyclic loading.

3 MEMORY HARDENING SURFACE MODEL BY CORTI ET AL. (2016)

In this original development, the hardening memory surface concept has been implemented within the Severn-Trent sand model (Gajo and Muir Wood, 1999). The addition of the hardening memory surface did not cause any modification to the original Severn-Trent sand model such that the monotonic response of the soil remains unvaried. The addition of the memory surface affects only the response under unloading or repeated loading (i.e. non-monotonic loading). The model is characterised by wedge type surfaces in the *q-p'* plane. In the π-plane all the model surfaces are characterised by an Argyris shape (Argyris et al. 1974).

The size (or strength ratio $M=q/p'$) of the bounding surface (F) is governed by the value of the state parameter ψ:

$$M = (1 - k\psi)M_{CS} \qquad (1)$$

where k is a model parameter, M_{cs} is the strength ratio at critical state, while ψ is defined as the difference between the current specific volume and the volume at critical state for the same mean effective stress p'.

Isotropic elasticity is assumed while the elasto-plastic response is governed by a hardening modulus of the following form:

$$H = \frac{b^2}{b_{max}B}\exp\left[\left(\frac{\mu b^M}{b}\right)(1 - k\psi)\right] \qquad (2)$$

where b and b^M are the distances of the current stress to the image on the bounding and memory surfaces respectively, b_{max} is the maximum value that b can assume, B is a modelling parameter of the original Severn-Trent sand model, while μ is the additional constitutive parameter governing the increase in stiffness within the memory surface. It should be noted that in this model stress distances are defined in the normalised stress plane $q/(1 - k\psi) - p'$.

The size (m^M) of the memory surface is governed by the following equation:

$$\delta m^M = \frac{z}{pn_q}\left[t\frac{H^M}{m_p}\delta\varepsilon_v^p - \frac{b_{max}^M - b^M}{\varsigma}\langle\delta\varepsilon_v^p\rangle\right] \quad (3)$$

where reference should be made to Corti et al. (2016) for the definition of the different symbols. However, it can be highlighted that expression (3) is composed by a first term governing the expansion of the surface (which does not require any additional parameter) and by a second term governing the shrinkage of the surface when dilative volumetric strains occur. This second mechanism is governed by the parameter ς.

The rule for the changing orientation (α^M) of the memory surface can be obtained by imposing an additional consistency condition for the image stress on the memory surface. For triaxial conditions the evolution law reduces to:

$$\delta\alpha^M = \frac{H^M}{m_{pn_q}}\delta\varepsilon_v^p - t\delta m^M \quad (4)$$

Comprehensive description of the model and definition of symbols can be found in Corti et al. (2016). A list and description of the twelve required parameters are provided in Table 1 where only the last two are relevant to the new hardening memory surface.

Table 1.List of model parameters Corti et al. (2016)

Parameter	Description
G	Elastic shear modulus
ν	Poisson's ratio
M_{cs}	Critical state stress ratio
λ	Slope critical state line υ-ln p' plane
υ_λ	Intercept critical state line υ-ln p' plane
R	Ratio of yield and bounding surface
B	Parameter hardening modulus
k	Parameter for strength - state parameter
A	Flow rule multiplier
k_d	State parameter and flow rule
μ	Hardening memory surface
ς	Damage memory surface

4 MEMORY HARDENING SURFACE MODEL BY LIU ET AL. (2018)

Liu et al. (2018) implemented the memory surface in the SANISAND 04 model of Dafalias and Manzari (2004). The model surfaces (yield, bounding and memory surfaces) are also open wedges. Differently from Corti et al. (2016), only the bounding surface is characterised by an Argyris type shape; the yield and the memory surface have a circular shape in the π-plane. The image points between surfaces are defined as those points with the same Lode angle θ. The hardening modulus has the following form:

$$H = \frac{b_0}{(\boldsymbol{r}-\boldsymbol{r_{in}}):\boldsymbol{n}}exp\left[\mu\left(\frac{p\prime}{p_{atm}}\right)^{n=0.5}\left(\frac{b^M}{b_{max}}\right)^2\right] \quad (5)$$

where reference should be made to Liu et al. (2018a) for the definition of all the symbols. Expression (5) has a rather similar form to Corti et al. (2016). However, there is a main difference in the inclusion of a mean effective stress dependent term $(p'/p_{atm})^{0.5}$ which will be particularly useful for capturing the influence of effective stress level on the plastic strain accumulation rate. The parameter μ has a similar function as in Corti et al. (2016) governing the stiffening inside the memory surface and in turn the progressive expansion during cyclic loading (which is linked to the development of plastic strains). The rules for the evolution of the memory surface (size and orientation, m^M and α^M respectively) are defined as follows

$$\delta m^M = \sqrt{\frac{3}{2}}\delta\boldsymbol{\alpha^M}:\boldsymbol{n} - \left(\frac{m^M}{\varsigma}\right)f_{shr}\langle\delta\varepsilon_v^p\rangle \quad (6)$$

$$\delta\boldsymbol{\alpha^M} = \frac{2}{3}\langle L^M\rangle h^M(\boldsymbol{r_\theta^b} - \boldsymbol{r^M}) \quad (7)$$

which have been derived in an analogous way as in Corti et al. (2016). The only additional parameter if compared to SANISAND 04 is the damage parameter ς in relationship (6). Liu et al. (2018a)

proposed also a further improvement to the dilatancy rule introducing a memory surface dependent term whose weight is governed by the parameter β:

$$D = A_0 exp\left(\beta \langle b_d^M \rangle / b_{ref}\right)(\boldsymbol{r_\theta^d} - \boldsymbol{r}) : \boldsymbol{n} \quad (8)$$

Full formulation of the model and definitions of the model symbols, including those in expression (8), can be found in Liu et al. (2018a). Overall the model requires the definition of 14 parameters given in Table 2 with the only last three inherent to the memory surface addition.

Table 2. List of model parameters Liu et al. (2018)

Parameter	Description
G	Elastic shear modulus
ν	Poisson's ratio
M_{cs}	Critical state stress ratio
λ_c	Critical state line shape parameter
ξ	Critical state line shape parameter
e_0	Critical void ratio
m	Yield locus opening parameter
n^d	Void ratio dependence parameter
h_0	Hardening parameter
c_h	Hardening parameter
A_0	Intrinsic dilatancy parameter
μ	Hardening memory surface
ς	Damage memory surface
$\boldsymbol{\beta}$	Dilatancy memory model parameter

5 MODEL CALIBRATION

Both models can be calibrated against experimental results on soil elements. The parameters related to the original Severn-Trent sand and SANISAND04 models can calibrated following the guidance of the original authors (Gajo and Muir Wood, 1999; Manzari and Dafalias 2004). For both memory surface models, the hardening parameter μ can be calibrated against the results of accumulated strains with number of cycles for drained triaxial tests. Figure 2 shows the calibration of the model of Liu et al. (2018a) against the experimental program carried out by Witchmann (2005) which have been used in this paper. Values of μ=260 is selected for the model by Liu et al. (2018), while μ=13 is calibrated for the model by Corti (2016) using an analogous procedure.

The damage parameter ς has generally little influence for drained cyclic test results and it is often calibrated against undrained cyclic tests. However, this parameter has also an influence on the cyclic response at high stress ratio as shown in Figure 3. As such the value was selected to be ς*=0.0005* for both Liu et al. (2018a) and Corti (2016).

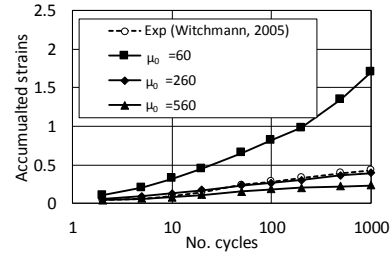

Figure 2 Calibration of the memory hardening parameter μ for the model of Liu et al. (2018a)

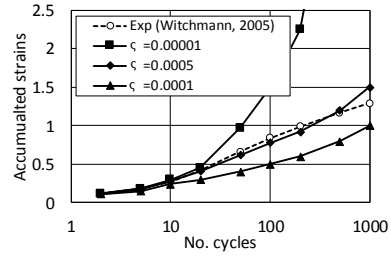

Figure 3 Influence of the damage parameter ς for the model of Liu et al. (2018a)

The model by Liu et al. (2018a) requires in addition the parameter β appearing in the new definition of the dilatancy coefficient D in Equation (8). This parameter mainly controls the post-dilation reduction of the mean effective stress in undrained tests. Larger values of β allow for larger reductions in mean effective pressure, possibly up to full liquefaction. Since the considered set of drained test results does not support the calibration of β, β = 1 has been set judiciously with negligible influence on the strain accumulation predicted during drained cyclic tests.

6 SIMULATIONS AND COMPARISON

The typical deviatoric stress - strain simulations for both models under drained cyclic loading are reported in Figure 4, where the progressive stiffening of the soil response with number of cycles is clearly visible.

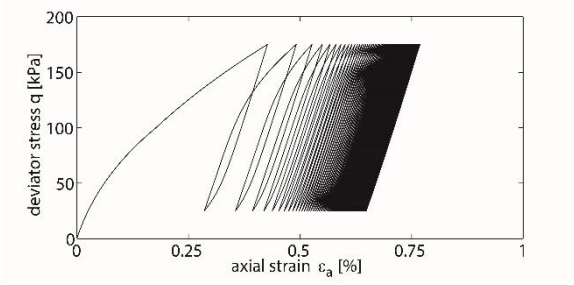

Figure 4 Deviatoric stress-strain response under drained cyclic loading for both models.

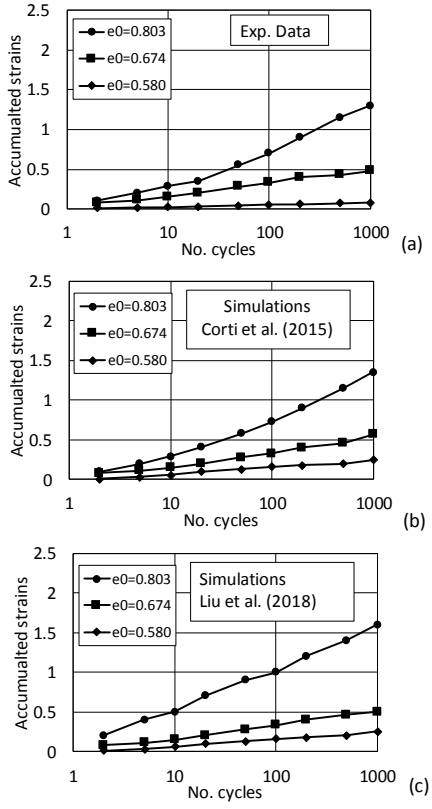

Figure 5 Influence of the initial void ratio on cyclic strain accumulation. Test/simulation settings: p_{in}= 200 kPa, η_{ave}= 0.75, q_{ampl}= 60 kPa.

The simulations of both models against the experimental results of Witchmann (2005) for triaxial cyclic loading on samples with different densities are provided in Figure 5. The simulations are carried out imposing up to 1000 loading cycles. Figure 5 shows that both models predict well the larger accumulated strains for looser material, although they appear to slightly overestimate the plastic strain accumulation for the densest configuration.

The model performances to simulate varying cyclic amplitudes are proposed in Figure 6. The model by Liu et al. (2018a) seems to better reproduce this feature and this is thought to be due to the introduction of a pressure-dependent term in the hardening modulus formulation (Eq.5)

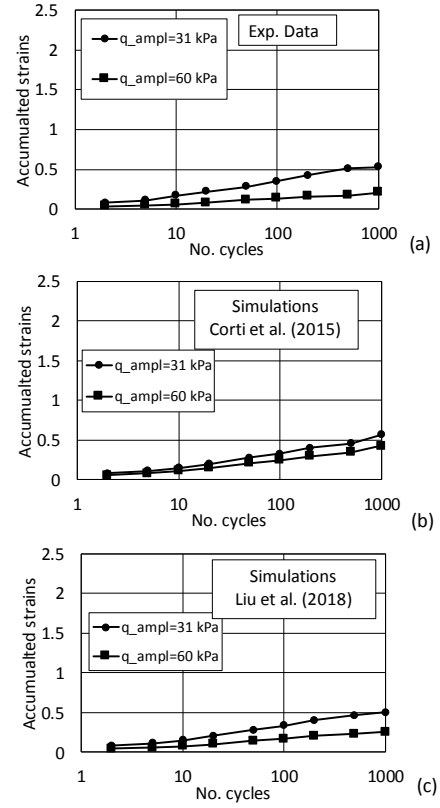

Figure 6 Influence of the cyclic amplitude on cyclic strain accumulation. Test/simulation settings: p_{in}= 200 kPa, η_{ave}= 0.75, e= 0.702.

The influence of the average cyclic stress ratio is shown in Figure 7. The model by Corti et al.

(2016) captures quite well the accumulation of strains for low stress ratio up to η_{ave} around 1. The strain accumulation for larger stress ratio is then underestimated. Conversely, the model by Liu et al. (2018a) overestimates the strain accumulation for high stress ratios. However, it should be noted that cyclic at such high stress ratios close or above critical state stress ratios may be rather rare. Experimental results may also be quite affected by errors (Escribano et al. 2018), therefore final conclusions cannot be drawn.

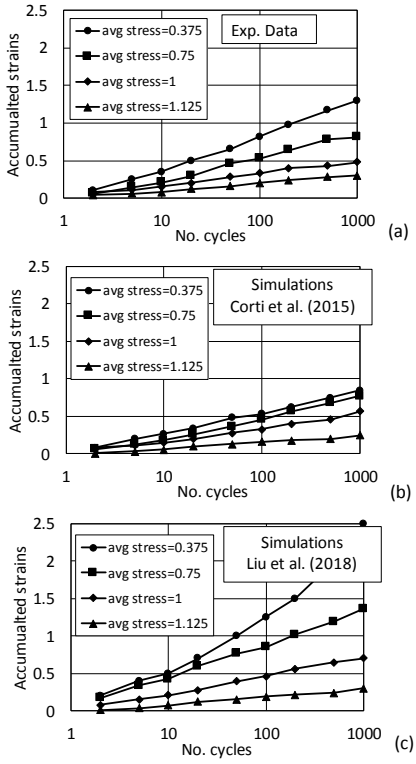

Figure 7 Influence of the average stress ratio on cyclic strain accumulation. Test/simulation settings: p_{in}= 200 kPa, q_{ampl}= 60 kPa, e= 0.702.

Finally, the improved performances of the Liu et al. (2018a) model due to the addition of the pressure dependent term in Eq.(5) are presented in Figure 8. This figure shows simulations with a power exponent *n* (see Eq.5) equal to 0 to reproduce independence from the mean effective stress (Figure 8b) and with a power exponent *n* of 0.5 (Figure 8c). The superior performance of this last set of simulations are clear. Such feature could be also implemented in Corti et al. (2016) as demonstrated in its further application to the sliding mud-mat foundation (Corti et al., 2017).

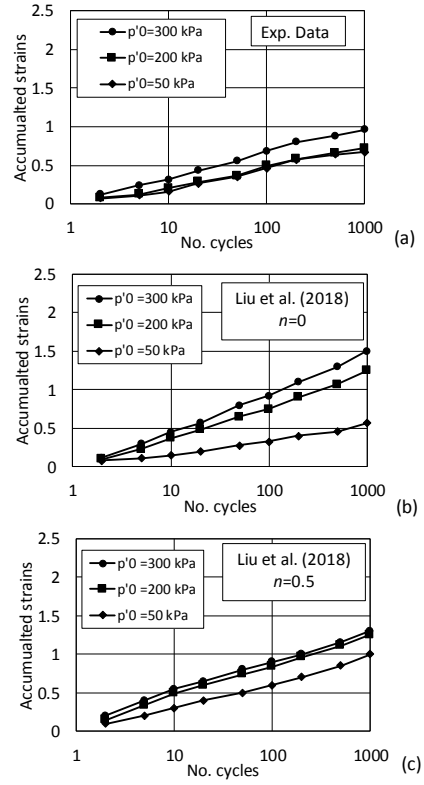

Figure 8 Influence of exponent n in Eq(5) to predict the pressure dependent behaviour. Test/simulation settings: η_{ave}= 0.75, q_{ampl}= 60 kPa, e= 0.702.

At the expense of an additional model parameter, Liu et al. (2018a) could also offer a slightly better simulation of the undrained cyclic response. The reader should refer to the Liu et al. (2018b) and to Liu et al. (2018a) where it is demonstrated that small adjustments of the parameter β permit the simulation of the full liquefaction behaviour and the achievement of almost zero mean isotropic effective stress.

7 CONCLUSIONS

This paper has shown that the implementation of the new hardening memory surface concept in

two different constitutive models resulted in superior capabilities for predicting the high cyclic behaviour of soils. Progressive soil stiffening and rate of plastic strains accumulation could be well predicted for a range of loading conditions. The direct comparison between the two models (Corti et al. 2016 and Liu et al. 2018a) demonstrated that the second has slightly better capabilities due to the addition of a pressure dependent term in the hardening modulus. At the expense of an additional model parameters introduced in the flow rule, Liu et al. (2018a) managed also to obtain improved simulation of the cyclic liquefaction response. Nevertheless, it would be feasible and it is recommended to implement such small changes in the formulation of Corti et al. (2016), as done for example in the application shown in Corti et al. (2017). The two models offer a valuable constitutive modelling tool to predict the high-cyclic behaviour of soils for a range of loading conditions, both in the triaxial and generalised multiaxial stress space.

8 REFERENCES

Argyris, J. H., Faust, G., Szimmat, J., Warnke, E. P., William, K. J. (1974). "Recent developments in the finite element analysis of prestressed concrete reactor vessels." *Nucl. Eng. Des.*, 28(1), 42–75.

Corti, R. (2016). Hardening memory surface constitutive model for granular soils under cyclic loading. *Ph.D. thesis, University of Bristol*.

Corti, R., Diambra, A., Muir Wood, D., Escribano, D. E. & Nash, D. F. (2016). Memory surface hardening model for granular soils under repeated loading conditions. *Journal of Engineering Mechanics*, DOI: 10.1061/(ASCE)EM.1943-7889.0001174.

Corti, R., Gourvenec, S. M., Randolph, M. F., & Diambra, A. (2017). Application of a memory surface model to predict whole-life settlements of a sliding foundation. *Computers and Geotechnics*, 88, 152-163. https://doi.org/10.1016/j.compgeo.2017.03.014

Chow, S. H., O'Loughlin, C. D., Corti, R., Gaudin, C., & Diambra, A. (2015). Drained cyclic capacity of plate anchors in dense sand: Experimental and theoretical observations. *Géotechnique Letters*, 5(2), 80-85. https://doi.org/10.1680/geolett.15.00019

Dafalias, Y. F. & Manzari, M. T. (2004). Simple plasticity sand model accounting for fabric change effects. Journal of Engineering mechanics 130, No. 6, 622–634.

Escribano, D. E., Nash, D. F. T., Diambra, A. (2018). Local and Global Volumetric Strain Comparison in Sand Specimens Subjected to Drained Cyclic and Monotonic Triaxial Compression Loading. *Geotechnical Testing Journa*l, 42(4), DOI: 10.1520/GTJ20170054.

Gajo, A., and Muir Wood, D. (1999b). "Severn-Trent sand: A kinematic hardening constitutive model: The q-p formulation." *Géotechnique*, 49(5), 595–614.

Houlsby, G., C. Abadie, W. Beuckelaers, & B. Byrne (2017). A model for nonlinear hysteretic and ratcheting behaviour. *International Journal of Solids and Structures* 120, 67–80.

Liu, H. Y., J. A. Abell, A. Diambra, & F. Pisano (2018a). A three-surface plasticity model capturing cyclic sand ratcheting. *Géotechnique* DOI: 10.1680/jgeot.17.P.307.

Liu, H. Y., Zygounas, F., Diambra, A., & Pisanò, F. (2018b). Enhanced plasticity modelling of high-cyclic ratcheting and pore pressure accumulation in sands. *Proc. 9th European Conference on Numerical Methods in Geotechnical Engineering* June 25-27, 2018, Porto, Portugal (p. 87). CRC Press.

Pasten, C., H. Shin, & J. C. Santamarina (2013). Long-term foundation response to repetitive loading. *Journal of Geotechnical and Geoenvironmental Engineering* 140(4), 04013036.

Wichtmann, T. (2005). Explicit accumulation model for non-cohesive soils under cyclic loading. *Ph. D. thesis, Inst. Grundbau und Bodenmechanik* Bochum University, Germany.